

Anaerobic dissolution rates of U(IV)-oxide by abiotic and nitrate-dependent bacterial pathways

Maria P. Asta^{1*}, Harry R. Beller^{2,3}, and Peggy A. O'Day^{1,4}

¹ Sierra Nevada Research Institute, University of California Merced, 5200 North Lake Road,
Merced, CA 95343, United States

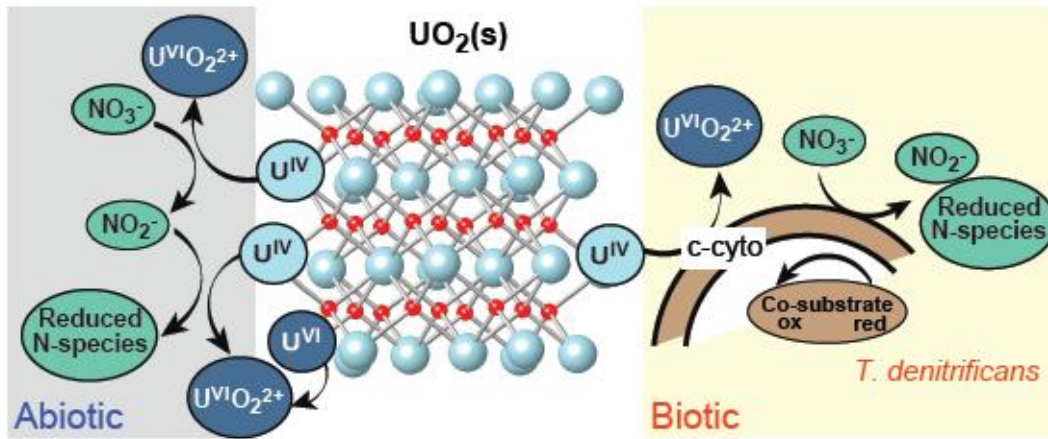
² Lawrence Berkeley National Laboratory, Berkeley, CA 94720, United States

³ Department of Chemical Engineering and Applied Chemistry, University of Toronto

⁴ Department of Life and Environmental Sciences, University of California Merced, CA 95343,
United States

*correspondence to: Maria-Pilar.Asta-Andres@univ-grenoble-alpes.fr; corresponding author present
address: Univ. Grenoble Alpes, Univ. Savoie Mont Blanc, CNRS, IRD, IFSTTAR, ISTerre, 38000
Grenoble, France

TOC Art



1 **ABSTRACT**

2 The long-term stability of U(IV) solid phases in anaerobic aquifers depends upon their
3 reactivity in the presence of oxidizing chemical species and microbial catalysts. We performed
4 flow-through column experiments under anaerobic conditions to investigate the mechanisms
5 and dissolution rates of biogenic, non-crystalline UO₂(s) by chemical oxidants (nitrate, nitrite),
6 or by *Thiobacillus denitrificans*, a widespread, denitrifying, chemolithoautotrophic model
7 bacterium. Dissolution rates of UO₂(s) with dissolved nitrite were approximately 5 to 10 times
8 higher than with nitrate alone. In the presence of wild-type *T. denitrificans* and nitrate, UO₂(s)
9 dissolution rates were similar to those of abiotic experiments with nitrite (from 1.15·10⁻¹⁴ to
10 4.94·10⁻¹³ mol m⁻² s⁻¹). Experiments with a *T. denitrificans* mutant strain defective in U(IV)
11 oxidation supported microbially mediated U(IV) oxidation. X-ray absorption spectroscopy
12 (XAS) analysis of post-reaction solids showed the presence of mononuclear U(VI) species
13 rather than as a solid phase. At steady state U release, kinetic and spectroscopic results suggest
14 detachment of oxidized U(VI) from the UO₂(s) surface as the rate-determining step rather than
15 electron transfer or ion diffusion. Under anaerobic conditions, production of nitrite by nitrate-
16 reducing microorganisms and enzymatically catalyzed, nitrate-dependent U(IV) oxidation are
17 likely dual processes by which reduced U solids may be oxidized and mobilized in the aqueous
18 phase.

19

20 Keywords: biogenic UO₂(s), anaerobic U(IV) dissolution rates, nitrate, nitrite, *Thiobacillus*
21 *denitrificans*

22

23

24 INTRODUCTION

25 Uranium (U) groundwater contamination is a worldwide environmental concern.
26 Stimulated *in situ* bioreduction of dissolved U(VI) and precipitation as a poorly soluble U(IV)
27 oxide (nominally $\text{UO}_2(\text{s})$) has received considerable attention as a remediation approach for
28 immobilizing U in aquifers under moderately reducing conditions (known as reductive
29 immobilization)^{1,2,3,4,5}. Nanoparticulate uraninite ($\text{UO}_{2+x}(\text{s})$)^{6,7} and non-crystalline disordered
30 U(IV) (monomeric and polymeric U(IV)-oxides)^{8,9,10} have been reported as the product of
31 microbially reduced U(IV). The presence of multiple U(IV) species has been reported in field
32 sediments^{5,11,12,13} and laboratory experiments¹⁴. Some of these studies proposed that uraninite
33 was the end product of abiotic reduction of U(VI)^{5,12}, which, in complex systems such as natural
34 sediments, may occur concomitantly with biological U(VI) reduction¹², whereas others
35 suggested precipitation of non-crystalline U(IV) species and transformation to nanocrystalline
36 uraninite with aging.^{14,15} Microbially mediated U(IV) oxidation under anaerobic conditions
37 may remobilize these U(IV) forms, and thus render long-term reductive immobilization less
38 effective.^{16,17,18,19,20,21} Therefore, identifying mechanisms and quantifying rates of U release
39 from re-oxidation and dissolution of $\text{UO}_2(\text{s})$ and related U(IV) solid-phase contaminants are
40 important for understanding potential U mobility in the environment.

41 Abiotic oxidation of $\text{UO}_2(\text{s})$ by molecular O_2 proceeds rapidly and oxidation rates have been
42 investigated under a variety of conditions, including variable pO_2 , pH, and dissolved inorganic
43 carbon and cations^{22,23}. Dissolution rates of $\text{UO}_2(\text{s})$ produced by microbial reduction (biogenic
44 $\text{UO}_{2+x}(\text{s})$) under anaerobic and aerobic conditions were found to be within experimental error
45 of those of chemically synthesized $\text{UO}_2(\text{s})$ in carbonate-free systems in one study²². Another
46 study proposed that chemogenic uraninite was more resistant to oxidation than forms of
47 biogenic U(IV)-oxides in the presence of dissolved oxygen²³. Monomeric forms of U(IV) have
48 been found to be less stable and more susceptible to oxidation than biogenic uraninite under

49 anoxic conditions²². However, Cerrato et al.²³ suggested that exposure of biogenic U(IV) solids
50 to oxidants and transport processes that control exposure and U release are more important than
51 the actual form of the solid, given relatively small differences observed in the oxidation rate
52 constants of biogenic uraninite and monomeric U(IV) in the presence of oxygen.

53 Anaerobic oxidation of U(IV) solids in the presence of dissolved nitrate (NO_3^-) and its
54 reduction products is of particular concern in subsurface U.S. Department of Energy sites and
55 other sites worldwide where U and nitrate are found as co-contaminants.^{17,24,25,26,27,28,29,30} In
56 anaerobic systems, the abiotic oxidation of $\text{UO}_2(\text{s})$ coupled to nitrate reduction in the absence
57 of iron was observed to be slow³¹. In the presence of nitrate-reducing and denitrifying
58 microorganisms, enzymatic reduction of nitrate may produce nitrite (NO_2^-), nitrous oxide
59 (N_2O), or nitric oxide (NO) species that may serve as abiotic oxidants for $\text{UO}_2(\text{s})$ and co-occur
60 with direct enzymatic oxidation of U(IV) by anaerobic, nitrate-reducing bacteria.

61 *Thiobacillus denitrificans* is a widely distributed and well-characterized obligate
62 chemolithoautotroph with a diverse metabolism³², capable of anaerobic, nitrate-dependent
63 U(IV) oxidation at circumneutral pH, as well as nitrate-dependent Fe(II) oxidation and coupled
64 oxidation of inorganic sulfur compounds, under either aerobic or denitrifying
65 conditions.^{18,32,33,34,35,36,37} Beller¹⁸ found that *T. denitrificans* was capable of anaerobic, nitrate-
66 dependent oxidative dissolution of synthetic and biogenic U(IV) oxides in batch laboratory
67 experiments; comparable U(IV) oxidation was not observed in killed controls or in no-nitrate
68 controls with live cells. The role of denitrification intermediates (NO_2^- , NO, N_2O) was not
69 explicitly investigated in that study, although nitrite was not detected (detection limit, 10 μM)
70 throughout the U(IV) experiment or in no-U(IV) controls that consumed 13 mM nitrate in 2 h.
71 Biochemical studies of *T. denitrificans* insertion mutants³⁸ strongly suggest that, at least for this
72 bacterium, direct enzymatic U(IV) oxidation under denitrifying conditions may have primacy
73 over secondary abiotic U(IV) oxidation by denitrification intermediates such as nitrite. A

74 mutant strain with a defective *Tbd_0187* gene (*Tbd_0187::kan*, also used in the present study)
75 had only 47% of wild-type U(IV) oxidation activity and 64% of wild-type denitrification
76 activity. However, when this mutant was complemented with an intact copy of the mutated gene
77 (in *trans*, on a plasmid), the U(IV) oxidation activity was restored to 130% of wild-type levels
78 but denitrification activity was not improved (55% of wild-type)³⁸. These results suggest that
79 the presence of the intact *c*-type cytochrome encoded by the *Tbd_0187* gene was more
80 important for U(IV) oxidation than the level of denitrification activity.

81 Although previous studies examined the dissolution of synthetic and biogenic U(IV) oxide
82 phases under a variety of conditions, quantification of reaction rates and comparisons between
83 different studies are challenging due to differences in experimental approach as well as in
84 reactant material^{39,40,41,42}. Comparisons between abiotic rates measured under sterile conditions
85 and those measured in the presence of U(IV)-oxidizing microorganisms are often complicated
86 by different experimental conditions needed to stimulate or maintain microbial activity. This
87 study differs from prior investigations in its direct comparison of U dissolution in the absence
88 and presence of a U(IV)-oxidizing model bacterium, *T. denitrificans*, and the addition of
89 dissolved nitrate, nitrite, or both using relatively simple reactant solutions (i.e., buffered pH and
90 carbonate-free solutions). Furthermore, our experiments employed flow through porous
91 medium (ground quartz) with a low solution volume in a strictly anaerobic environment, rather
92 than a batch or tank system in which the solution:solid ratio is high. This flow-through system
93 provided a more realistic water:solid ratio with the advantage of removing dissolved species
94 that may influence reaction rate or solubility of mineral phases⁴³, and thus better simulated the
95 dynamic porewater flow regime of saturated subsurface environments.

96 MATERIALS AND METHODS

97 **Biogenic UO₂(s) synthesis.** Multiple batches of U(IV)-oxide (hereafter referred to as UO₂(s))
98 were produced by reduction of dissolved U(VI) by *Shewanella oneidensis* strain MR-1

99 following published methods.^{6,44} *S. oneidensis* was grown in lysogeny broth (LB) under aerobic
100 conditions. Cells were separated by centrifugation and washed with a buffer containing 30 mM
101 NaHCO₃, 20 mM PIPES, and 20 mM lactate (pH 6.3) under anaerobic conditions (10% H₂,
102 90% Ar headspace). Solids were resuspended in the same solution amended with 1500 μM of
103 uranyl acetate. After U(VI) reduction and precipitation of UO₂(s), solid particles were cleaned
104 by resuspending the solids in 1 M NaOH for 12 h. Solids were then centrifuged and resuspended
105 in anaerobic hexane for 12 h to separate UO₂(s) from biomass. Finally, the solids were
106 centrifuged and stored under anaerobic conditions in a 1 M NaHCO₃ solution. All cultures and
107 subsequent experiments were maintained under strict anaerobic and sterile conditions.

108 **Dissolution experiments.** Dissolution of UO₂(s) in column flow-through experiments in the
109 absence or presence of *T. denitrificans* was performed under anaerobic conditions at room
110 temperature (25±1 °C) in an anaerobic glove box (Type A, Coy Laboratory Products, Inc., Grass
111 Lake, MI). The entire experimental set-up (input and output solutions, peristaltic pump, flow-
112 through reactors, and tubing) was enclosed in the glove box (25±1 °C) and purged with a gas
113 composition of 90% N₂ and 10% H₂. Ultrapure water (18.2 MΩ·cm, Milli-Q Plus, Millipore)
114 used to prepare the input solutions was boiled before use to remove dissolved oxygen, cooled
115 in the anaerobic glove box, and left for at least 24 h before performing experiments. Oxygen
116 partial pressure in the glove box was continuously monitored with a gas analyzer (Model 10,
117 Coy Laboratory Products) and read 0 ppm during the experiments. All material (tubes, quartz,
118 solutions, columns, etc.) was sterilized before each experiment and equilibrated in the anaerobic
119 glove box before use.

120 Flow-through column experiments were carried out by packing a mixture of UO₂(s) with
121 ground natural quartz (~200-500 μm from Unimin, Inc. and treated to clean surface impurities)
122 into either 1-mL (0.8-cm ID x 2-cm length) or 5-mL (1.3-cm ID x 4.5-cm length) polypropylene
123 chromatography columns (SUPELCO) and protected from light exposure. The final mixtures

124 contained average concentrations of 570 mg U/kg of quartz to 170 mg U/kg of quartz for the 1-
125 mL and 5-mL columns, respectively. Influent solutions were filtered with a 0.2- μ m
126 polycarbonate filter (Millipore) at both the inlet and outlet ends of the column. Flow was
127 directed upward in the experiments to minimize bubbles (e.g., N₂ from denitrification) and was
128 controlled with an HPLC pump (Ismatec C.P. 78001-02), which had a variation of less than
129 3%. Influent flow rates were gravimetrically determined. Influent dissolved oxygen and pH
130 were measured periodically by electrode (Orion 081010MD for dissolved oxygen and Thermo
131 Scientific Orion 9102DJWP for pH). In selected experiments, effluent pH was monitored in
132 line with a Thermo-Scientific Orion 9102DJWP pH electrode.

133 For abiotic dissolution experiments, quartz and UO₂(s) were mixed under anaerobic
134 conditions, then 1 mL of 10 mM NaCl (pH 7) was added to the mixture and packed into
135 columns. For biotic experiments, *T. denitrificans* cells were harvested anaerobically by
136 centrifugation in sealed polycarbonate bottles, washed once under anaerobic conditions, and
137 resuspended in anaerobic 10 mM NaCl (pH 7). The optical density at 600 nm (OD₆₀₀) of this
138 solution was adjusted to 2 (ca. 1.8 x 10⁹ cells·mL⁻¹) by diluting with the same NaCl solution, 1
139 mL was added to the mixture of quartz and UO₂(s), and the slurry was immediately loaded into
140 the columns (details of the cultivation and incubation of *T. denitrificans* can be found in the
141 Supporting Information). In order to confirm that the process was enzymatically mediated, in
142 addition to wild-type *T. denitrificans*, a mutant *T. denitrificans* strain that was ~50% defective
143 in U(IV) oxidation activity (relative to wild-type) was used that had an insertion mutation in
144 the *Tbd_0187* gene, which encodes a *c*-type cytochrome shown to be involved in anaerobic
145 U(IV) oxidation³⁸.

146 Influent solutions for dissolution experiments were prepared by mixing reagents (ACS-
147 grade or better NaNO₃, NaNO₂, NaCl, and MOPS as a pH buffer) with the deoxygenated
148 ultrapure water. Solutions were made with variable nitrate, nitrite, and chloride concentrations

149 to maintain an approximately constant ionic strength (Table S1). The pH was adjusted to ~7 by
150 adding NaOH (2 M) (Table S1). Solids were reacted with influent solutions (Table S1) for ~2-
151 5 days and column effluent was collected using a multi-channel fraction collector
152 (Spectra/Chrom® CF-1).

153 **Uranium dissolution rates.** The $\text{UO}_2(\text{s})$ dissolution rate, R , ($\text{mol m}^{-2} \text{s}^{-1}$), was calculated
154 according to the following expression (Eq. 1):^{41,45}

$$155 \quad R = \frac{[U]_{\text{ss}} \times Q}{V \times A \times [\text{UO}_2(\text{s})]} \quad \text{Eq. 1}$$

156 where, assuming that the U concentration in the input solution is zero and the U released is due
157 to $\text{UO}_2(\text{s})$ dissolution, $[U]_{\text{ss}}$ is the concentration ($\text{mol U} \cdot \text{L}^{-1}$) in the effluent solution at steady-
158 state, A is the specific surface area ($\text{m}^2 \cdot \text{g}^{-1}$), V is the estimated pore volume (L), $[\text{UO}_2(\text{s})]$ is
159 the $\text{UO}_2(\text{s})$ solid concentration in the reactor ($\text{g} \cdot \text{L}^{-1}$), and Q is the volumetric flow rate through
160 the system ($\text{L} \cdot \text{s}^{-1}$) (Table S2). The $[U]_{\text{ss}}$ was the average concentration of 20 and 100 or more
161 pore volumes eluted for the 5-mL and 1-mL columns, respectively, over which the effluent U
162 concentration varied $\leq 15\%$. The error associated with the dissolution rate was estimated by
163 propagation of the uncertainty in each of the terms in Eq. 1 (Table S2) and ranged from 6-27%.
164 The estimated error was dominated by the uncertainty of the mass concentration of U in the
165 steady-state ($[U]_{\text{ss}} \leq 15\%$) and the uncertainty of the mass measurements (2-24%).

166 **Analytical methods.** Detailed information about aqueous and solid analytical methods are
167 presented in the Supporting Information. Briefly, column effluent solutions were analyzed for
168 total U by ICP-MS (Agilent 7500cs); the detection limit was $4.2 \times 10^{-5} \mu\text{M}$ (10 ppt) and
169 analytical precision was $< \pm 5\%$. We attempted to measure U(VI) speciation by kinetic
170 phosphorescence analysis (KPA), but concentrations were below detection after dilution to
171 reduce quenching from dissolved ions. Nitrate and nitrite were determined
172 spectrophotometrically with a Cary-300-Bio spectrophotometer. $\text{UO}_2(\text{s})$ was characterized by
173 X-ray diffraction (XRD) on a PANalytical X'pert Pro diffractometer. Scanning electron

174 microscopy (SEM) and TEM images were obtained using a FEI Quanta 200 ESEM and a JEOL-
175 JEM-2010 HRTEM, respectively. The surface area was measured using 7-point N₂ adsorption
176 isotherms with a Micrometrics Tri-Star 3000 surface area analyzer. Uranium L_{III}-edge X-ray
177 absorption spectroscopy (XAS) data, including X-ray absorption near edge structure (XANES)
178 and extended X-ray absorption fine structure (EXAFS) spectra, were collected at the Stanford
179 Synchrotron Radiation Lightsource (SSRL, California, USA) beamlines 11-2 and 4-1.

180 RESULTS

181 **Characterization of unreacted biogenic UO₂(s).** Powder XRD patterns of biogenic UO₂(s)
182 showed weak reflections that matched the major reflections of crystalline UO₂(s), but with
183 significant broadening, lower amplitude, and lower signal-to-noise ratio (Figure S1). These
184 features are similar to those of biogenic UO₂(s) produced in other studies and are attributed to
185 small particle size, low crystallinity, and/or structural disorder^{6,46}. The surface area of freeze-
186 dried UO₂(s) was measured by the N₂-BET method on two batches of UO₂(s) (Table S1), with
187 a mean surface area of 72.81±0.69 m²g⁻¹. Examination of unreacted UO₂(s) particles by SEM
188 showed particle aggregates of up to several micrometers in diameter (Fig. S2a, S2b). Lattice
189 fringes of particles observed by TEM images indicated individual particles of 2-4 nm in
190 diameter (Fig. S2c), consistent with other studies of biogenic UO₂(s) produced by the method
191 described above⁴¹. Results from XRD and TEM, and from XAS analysis (discussed below),
192 support the interpretation that the majority of the biogenic starting material was mostly
193 nanoparticulate UO₂(s).

194 **Flow-through column abiotic experiments.** The abiotic dissolution of UO₂(s) was examined
195 in the presence of nitrate and/or nitrite (0-20 mM) in buffered solutions at circumneutral pH
196 (7.0-7.3). Total U concentrations in column effluent normalized to the total molar mass of
197 UO₂(s) added to the column in the abiotic experiments are shown in Figure 1. At the beginning
198 of all the experiments, an initial peak of effluent U was observed, which is a common

199 phenomenon in flow-through experiments that is attributed to labile U(VI) on the UO₂ surface⁴⁷
200 or to the passage of colloidal U through the filter membrane during the first flush⁴¹. Therefore,
201 the dissolution rate was calculated once a steady state in effluent U concentration was attained.
202 The results display differences in the total amount of U released, and therefore, in the amount
203 of U dissolved, depending on the influent composition (Figure 1, Table S2). In the absence of
204 an oxidant, the effluent U in replicate columns with anaerobic NaCl solutions buffered at pH
205 ~7 remained low and relatively constant (Figure 1a). The calculated average U dissolution rate
206 ($1.05 \cdot 10^{-14}$ mol m⁻² s⁻¹) is similar to the lowest rate reported by Ulrich et al.⁴¹ for biogenically
207 precipitated UO₂(s) (Table 1). The addition of 20 mM nitrate to the influent solution resulted in
208 an increase in the average dissolution rate ($3.02 \cdot 10^{-14}$ mol m⁻² s⁻¹) compared to that of
209 experiments in the absence of an oxidant (Figure 1b). In contrast, when the columns were
210 supplied with nitrite, the mass-normalized U effluent concentrations and calculated steady-state
211 dissolution rates were higher than in the presence of nitrate alone (Figure 1, Table S2). The
212 dissolution rates with mixtures of nitrate and nitrite were similar to those obtained with nitrite
213 only, which is consistent with the expected stronger effect of nitrite as an oxidant in abiotic
214 UO₂(s) dissolution compared to nitrate (Figure 1d-f, Figure S3, Table S2).

215 **Flow-through column experiments in the presence of *T. denitrificans*.** Dissolution of UO₂(s)
216 in the presence of *T. denitrificans* and dissolved nitrate (\pm nitrite) was compared to abiotic rate
217 experiments. Replicate experiments always included an abiotic control column run
218 simultaneously with the same influent solution as the biotic columns (Table S2). In most
219 experiments, columns with *T. denitrificans* showed rates of UO₂(s) dissolution of about one
220 order-of-magnitude faster than those of the simultaneous abiotic control experiment (Figure 2,
221 Table S2). However, in a few simultaneous replicate columns, UO₂(s) dissolution rates were
222 lower and closer to those of abiotic controls (e.g. B1-R2, B2-R3, and B4-R1, Table S2) and
223 nitrite concentrations (Figure S4) were below detection limit (B1-R2), slightly lower (B2-R3)

224 than the biotic replicates, or followed the same trend as the control experiment (B4-R1), which
225 could indicate low or no enzymatic oxidation. Overall, $\text{UO}_2(\text{s})$ dissolution rates were more
226 variable in experiments with *T. denitrificans* than in abiotic experiments, and a relatively
227 constant effluent U concentration was sometimes not observed until near the end of the
228 experiment. Nitrite concentrations measured in the effluent solutions of experiments with *T.*
229 *denitrificans* with nitrate (but no added nitrite) were higher (~20-160 μM) than in abiotic nitrate
230 control experiments (~5-10 μM), demonstrating microbially accelerated conversion of nitrate
231 to nitrite (Figure S4). Furthermore, in two control column experiments with *T. denitrificans* and
232 quartz but no $\text{UO}_2(\text{s})$, solutions with influent nitrate concentrations of 1 or 10 mM produced
233 effluent nitrite concentrations near the limit of detection (0.42 μM) (data not shown). Overall,
234 abiotic dissolution rates measured in experiments with added nitrite were similar to rates
235 observed in experiments with *T. denitrificans* and added nitrate (Table 1).

236 Column experiments were performed with a mutant strain of *T. denitrificans* that was
237 previously shown to be ~50% defective in U(IV) oxidation.³⁸ Results showed a decrease in the
238 average $\text{UO}_2(\text{s})$ dissolution rate of 44% compared to that of experiments with the wild-type
239 strain. The decrease in dissolution rate was smaller (34% rather than 44%) if effluent U
240 concentrations were compared with those of simultaneous abiotic control columns with the
241 same influent nitrate concentration (10 mM) (e.g., controls B3b-CT6 and B5-CT8 in Figure 2c
242 and 2e, respectively) (Table 1, Figure 2). The differences in rate exceeded the estimated
243 propagated error for these experiments (Table 1). This result supports the role of enzymatic
244 mediation by *T. denitrificans* in the U(IV) oxidation process (Figure 2).

245 **X-ray absorption spectroscopy of unreacted and reacted $\text{UO}_2(\text{s})$.** Because of the low
246 concentrations of U and the presence of quartz in the reacted columns (which added background
247 noise), XAS data were limited to mostly XANES spectra, with usable EXAFS spectra obtained
248 for only three reacted samples. XANES spectra of $\text{UO}_2(\text{s})$ samples and reference compounds at

249 the U L_{III}-edge are shown in Figure S5. The absorption maximum for U(IV) is found at 17,176
250 eV, which is ~2.7 eV lower in energy than the maximum for U(VI). U(VI)-oxide compounds
251 show a shoulder at approximately 17,191 eV, which has previously been shown to result from
252 multiple scattering resonances of the linear uranyl ion structure, specifically due to the short U-
253 O_{ax} bonds^{48,49}. Best fits of linear combinations of unreacted UO₂(s) and schoepite
254 [(UO₂)₈O₂(OH)₁₂·12(H₂O)] as a U(VI) reference compound showed that spectra were
255 dominated by unreacted material (72-100% ±10% in normalized spectra) with a small fraction
256 of U(VI) present in the solids (Figure S5, Table 2). Experiments performed with nitrite had the
257 highest uranyl fraction among the abiotic samples analyzed by XAS, although results were
258 variable among all columns. For columns reacted in the presence of *T. denitrificans*, the highest
259 U(VI) fractions [28% U(VI) in B1(R2) and 26% U(VI) in B3b(R2)] were in experiments with
260 nitrate (4 or 10 mM, respectively) that were run for longer duration (cumulative fluid volumes
261 of 647 and 776 mL, respectively; Table S2), although fit results were again variable.

262 Quantitative fits of EXAFS spectra of two unreacted UO₂(s) samples (Unr-1 and Unr-3)
263 indicated a local atomic environment around U consistent with the UO₂(s) structure⁶ (Figure 3,
264 Table S3). As noted in prior studies, atomic backscattering amplitudes in EXAFS of biogenic
265 nanoparticulate UO₂(s) tend to be lower than in crystalline U compounds, particularly for atoms
266 beyond the first bonded shell of O atoms, due to small particle size, local disorder, and in some
267 cases a component of monomeric U(IV) species.^{50,6,8,51,9,23} Backscattering from U-U shells at
268 interatomic distances of ~ 5.46 and 6.73 Å were not significant in the EXAFS spectrum of Unr-
269 1 (Figure 3), which may indicate a small difference in particle size or crystallinity, and/or a
270 variable fraction of monomeric U(IV), a common product of enzymatic U(VI) reduction in the
271 natural environment^{52,53,54} and laboratory studies⁵⁵, in addition to nanoparticulate
272 UO₂(s).^{50,8,51,23} In reacted column samples, XANES analysis indicated a low fraction of U(VI)
273 (< 30%), so the three EXAFS spectra were examined for evidence of backscattering from near-

274 neighbor axial oxygen atoms (O_{ax}) in the uranyl group (UO_2^{2+}) at interatomic distances from ~
275 1.74 to 1.83 Å (Table S4), in addition to O atoms at distances indicative of unreacted $UO_2(s)$
276 (2.30-2.35 Å). Quantitative EXAFS fits of reacted samples A2 (abiotic with 20 mM nitrite) and
277 B2 (with *T. denitrificans* and 5 mM nitrate) showed no evidence for O_{ax} backscattering or U-O
278 backscattering at distances other than expected for U-O in $UO_2(s)$. Fit results were similar to
279 those found for the U-O and U-U shells for Unr-1 and Unr-3 (Table S3). In the EXAFS fit of
280 reacted sample A9(R2) (abiotic with 18 mM nitrate + 10 mM nitrite), weak backscattering from
281 O_{ax} (at 1.77 Å) was permissible although backscattering at distances characteristic of U(VI) and
282 equatorial O atoms ($U-O_{eq}$), which span a range of distances, could not be distinguished in the
283 fit from O atoms in $UO_2(s)$ (Figure 3, Table S3). This column was reacted at a high nitrate +
284 nitrite concentration (28 mM) and with a higher cumulative pore volume than abiotic column
285 A2 (285 vs. 220 mL). Overall, the XAS results showed that U in reacted columns mostly
286 resembled unreacted $UO_2(s)$, but suggested evidence for a minor fraction of U(VI), with slightly
287 more U(VI) at high oxidant concentrations and longer reaction times. The lack of molecular-
288 scale evidence for interatomic scattering indicative of uranyl oxyhydroxide minerals suggests
289 the formation mostly of U(VI) surface complexes. If U(VI)-oxide solid phases were present,
290 their fraction was below detection by XAS.

291 **DISCUSSION**

292 **Abiotic and biotic rates of anaerobic $UO_2(s)$ dissolution.** Dissolution rates of $UO_2(s)$ at
293 steady-state U release as a function of nitrate and nitrite concentration, and in the absence and
294 presence of *T. denitrificans*, are compiled in Figure 4. In the absence of an oxidant, the average
295 $UO_2(s)$ dissolution rate ($1.05 \cdot 10^{-14} \text{ mol m}^{-2} \text{ s}^{-1}$) was similar to the slowest rates published
296 previously for bio- $UO_2(s)$ at neutral pH in carbonate-free solutions ($1.07 \cdot 10^{-14}$ to $3.42 \cdot 10^{-13} \text{ mol}$
297 $\text{m}^{-2} \text{ s}^{-1}$)⁴¹ (Table 1). Abiotic dissolution of $UO_2(s)$ by nitrate alone was relatively slow ($2.51 \cdot 10^{-}$
298 14 to $4.61 \cdot 10^{-14} \text{ mol m}^{-2} \text{ s}^{-1}$), although slightly faster than without addition of an oxidant, and not
299 dependent on nitrate concentration (4-20 mM NO_3^-) (Figure 4). These rates, measured at pH

300 7.0-7.3, are approximately two orders of magnitude slower than the rate reported by Ulrich et
301 al.⁴¹ for dissolution of synthetic UO₂(s) in the presence of 1 mM nitrate at pH 8 ($4.03 \cdot 10^{-12}$ mol
302 m⁻² s⁻¹; Table 1). Ulrich et al.⁴¹ obtained slower dissolution rates for bio-UO₂ than for synthetic
303 UO₂ solids (Table 1), although these differences were estimated to be within their experimental
304 error. With the addition of nitrite as an oxidant (with or without nitrate), UO₂(s) dissolution
305 rates were about 5 to 10 times higher than with nitrate alone, with the exception of one
306 experiment at low nitrite and nitrate concentrations (Figure 4, Figure S3, Table 1). Prior studies
307 have pointed out that nitrite, a product of nitrate reduction, is more reactive than nitrate and
308 could abiotically oxidize U(IV).^{16,17} To our knowledge, however, no anaerobic UO₂(s)
309 dissolution rates in the presence of nitrite under flow conditions have been reported previously.
310 In the absence of microbial activity, our experiments show the ability of nitrite to accelerate
311 UO₂(s) dissolution compared with nitrate, although there was not a strong dependence on
312 influent nitrite concentration over the range used in our experiments (0.08-20 mM; Figure S3).
313 Rates of UO₂(s) dissolution in the presence of *T. denitrificans* with nitrate (and with 0.08 mM
314 nitrite in one set of experiments) were generally higher than those for abiotic experiments with
315 nitrate-only, but similar to the range observed for abiotic experiments with nitrite (Figure 4).
316 Experiments with a mutant strain of *T. denitrificans* that is partially defective in U(IV)
317 oxidation³⁸ showed a decrease in average dissolution rate compared to rates from experiments
318 with wild-type *T. denitrificans* and the same concentration of influent nitrate, providing
319 evidence of enzymatically catalyzed U(IV) oxidation by *T. denitrificans*. Effluent U
320 concentrations in biotic experiments ranged from ~1-40 nanomolar, compared to effluent nitrite
321 of ~5-150 micromolar from the reduction of nitrate, with no apparent correlation between
322 effluent U and nitrite concentration, which was variable among biotic experiments (Figure S4).
323 Therefore, U(IV) alone could not have served as the dominant electron donor for nitrate
324 reduction by *T. denitrificans*. These observations support previously reported batch studies of

325 $\text{UO}_2(\text{s})$ oxidation by *T. denitrificans* indicating that nitrate reduction is coupled to a primary
326 electron donor other than U(IV) (e.g., H_2 from the glove box atmosphere).¹⁸ In fact, nitrate-
327 dependent U(IV) oxidation catalyzed by *T. denitrificans* has been reported to have a co-
328 metabolic dependence on H_2 oxidation.¹⁸

329 **Mechanisms of anaerobic $\text{UO}_2(\text{s})$ dissolution.** Under anaerobic conditions in the absence of
330 oxidants, radiolysis products such as H_2O_2 and O_2 from alpha decay of U reacting with water
331 molecules can oxidize U(IV) to produce surface species of U(V) or U(VI)^{22,41,56,57,58,59}. In early
332 studies, Bruno et al.³⁹ assumed that detachment of a hydroxo-U(IV) species ($\text{U}(\text{OH})_x^{(4-x)+}$) was
333 the rate-determining step in thin-film, flow-through dissolution experiments of synthetic $\text{UO}_2(\text{s})$
334 under reducing conditions. In our experiments, U(IV) oxidation attributed to radiolysis should
335 be relatively small given the short time-scale (minutes to hours), but is probably not negligible.
336 Total U concentration, rather than U species, was measured in effluent solutions, and therefore
337 we do not have direct knowledge of U aqueous speciation. In the absence of an oxidant
338 (experiments with NaCl solution), it is possible that U release from $\text{UO}_2(\text{s})$ surfaces was a
339 combination of dissolved U(IV) and U(VI) species from reaction with oxidants, such as H_2O_2
340 from the radiolysis of water.

341 In anaerobic systems, the abiotic oxidation of $\text{UO}_2(\text{s})$ coupled to nitrate reduction is
342 slow^{16,18}. Slightly faster $\text{UO}_2(\text{s})$ dissolution rates in the presence of dissolved nitrate compared
343 to experiments with NaCl only may be explained by adsorption of nitrate and direct oxidation
344 of $\text{UO}_2(\text{s})$, or radiolysis of nitrate to produce nitrite or other reactive NO_x species⁶⁰ at the $\text{UO}_2(\text{s})$
345 surface and acceleration of U(IV) oxidation and U(V) or U(VI) release. Both nitrate and
346 chloride form weak complexes in solution with U(IV) of similar thermodynamic affinity (Table
347 S5), and thus their sorption behavior on $\text{UO}_2(\text{s})$ is probably similar. Dissolution experiments
348 showed no dependence on nitrate concentration, and XANES analysis of one abiotic sample
349 (A5) reacted with 20 mM nitrate (and no nitrite or NaCl) showed only U(IV) in the solids after

350 reaction. These observations indicate that direct U oxidation by nitrate, or radiolysis to nitrite
351 (or other reduced N species) followed by U oxidation, is a weak effect. Aqueous complexes of
352 U(IV) with nitrate or chloride are orders-of-magnitude weaker than U(IV)-hydroxo complexes
353 (Table S5), and the latter are expected to be the stable U(IV) species detaching from the UO₂(s)
354 surface in the absence of U oxidation³⁹. Slightly faster UO₂(s) dissolution rates with nitrate
355 compared to chloride at similar concentrations are indirect evidence of surface oxidative
356 dissolution because, if detachment of U from the surface through formation of U(IV)-hydroxo
357 complexes were rate-determining, then observed rates in the presence of either chloride or
358 nitrate at constant pH should overlap. If nitrate adsorption accelerates surface oxidation of
359 U(IV) to U(VI) by either of the mechanisms described above, then detachment of uranyl-
360 hydroxo complexes would be rate-determining, and rates would be higher with more surface
361 oxidation. This mechanism relies on surface enhancement of UO₂(s) dissolution, since the
362 concentration of nitrate (1-20 mM) would be too low for radiolysis reactions to be important in
363 bulk solution.⁶⁰ The lack of dependence of the dissolution rate on nitrate concentration is
364 consistent with a surface mechanism that involves nitrate adsorption and detachment of an
365 oxidized U product, perhaps in addition to a U(IV) species, but it is a relatively small effect
366 overall (Figure 4).

367 Nitrite is a more effective oxidant of U(IV) than nitrate, with dissolution rates in abiotic
368 experiments about 5 to 10 times faster than with nitrate, and similar to average rates measured
369 in biotic experiments (Figure 4). In abiotic experiments with nitrite (\pm nitrate) or biotic
370 experiments with nitrate, bulk XANES analysis indicated that a low fraction of total U (3-19%)
371 was retained in the column as oxidized U(VI), with higher fractions (up to 32%) observed for
372 experiments of longer duration. These results are consistent with the presence of some adsorbed
373 or surface U(VI), or perhaps some U(V) that is not detectable by XANES²². EXAFS analysis
374 showed the lack of formation of an oxidized U(VI) phase (e.g., schoepite) as a surface coating,

375 which was proposed in other studies of $\text{UO}_2(\text{s})$ dissolution^{22,61}, probably due to the short time
376 scale of our experiments (3-5 days) and relatively slow rates of oxidation, or to the mobilization
377 of desorbed U(VI) species in our flow-through columns. The presence of surface U(VI) in
378 similar proportions in both biotic and abiotic experiments, and the observation that dissolution
379 rates are independent of nitrite concentration, support the hypothesis that the rate-determining
380 step at steady-state release is detachment of oxidized U(VI) from the $\text{UO}_2(\text{s})$ surface rather than
381 electron transfer or ion diffusion.

382 In *T. denitrificans*, two membrane-associated, *c*-type cytochromes that are involved in
383 anaerobic U(IV) oxidation were previously identified by Beller et al.³⁸ The similarity between
384 abiotic experiments with nitrite and biotic experiments with nitrate suggests a close interplay
385 of molecular and enzymatic electron transfer among N and U species. In experiments with *T.*
386 *denitrificans*, it is likely that U(IV) oxidation takes place *via* both the membrane-associated *c*-
387 type cytochrome (enzymatic) pathway previously described³⁸, and as a secondary abiotic
388 reaction with denitrification intermediates (e.g., nitrite, nitric oxide, nitrous oxide), with the
389 relative proportions of each pathway varying during the experiments. Steady-state rates were
390 estimated from U effluent concentrations towards the end of the experiments after formation of
391 a fraction of U(VI) in the columns (detected by XAS), presumably as a surface species. The
392 observed biotic and nitrite-catalyzed rates in this study are similar to dissolution rates measured
393 for the uranyl oxyhydroxide minerals Na-compreignacite ($R = 3.71 \cdot 10^{-13} \text{ mol m}^{-2} \text{ s}^{-1}$; $\log R = -$
394 12.43) and K-compreignacite ($R = 1.28 \cdot 10^{-13} \text{ mol m}^{-2} \text{ s}^{-1}$; $\log R = -12.89$) at pH 6.6-6.8 and low
395 dissolved carbonate concentrations using a similar experimental set-up of flow-through, quartz-
396 packed columns⁶². In that study, the authors noted that despite ion exchange during the
397 experiments, mineral dissolution rates were relatively insensitive to the interlayer cation
398 identity because the molecular-scale rate-determining step was the detachment of the uranyl
399 group from the mineral surface^{63,64,65}. The similarity in observed rates may indicate that uranyl

400 detachment from the surface is a common controlling mechanism when a steady-state surface
401 concentration of oxidized U is achieved.

402 **Environmental Implications.** Reduced U forms, including crystalline uraninite and
403 amorphous U(IV)-oxides, are susceptible to reoxidation^{5,20,66,14} and pose challenges to long-
404 term stability of U(IV) in aquifer sites remediated by reductive immobilization. This is mainly
405 due to groundwater influxes continuously introducing U(IV)-oxidizing species (e.g., O₂, NO₃⁻,
406 and NO₂⁻). Of these species, one of the most relevant for contaminated subsurface
407 environments at nuclear sites is nitrate, a common co-contaminant with uranium at U.S.
408 Department of Energy (DOE) sites^{16,24,67}. Nitrate inputs to aquifers have been observed to
409 threaten U(IV) stability, not only at nuclear sites, but also in areas unaffected by nuclear
410 activities^{28,29,30}. Although O₂ is a stronger oxidant^{22,68,69}, this study showed that oxidative
411 dissolution of reduced U under anaerobic conditions is accelerated substantially by the addition
412 of dissolved nitrite, or by a denitrifying chemolithoautotroph, *T. denitrificans*, that is pervasive
413 in aquifers and soils, together with nitrate (log rates from -13.94 to -12.31 mol m⁻² s⁻¹). *T.*
414 *denitrificans* or closely related species are prominent members of microbial communities at
415 some uranium-contaminated sites^{18,70,71,37}. In the environment, nitrite is a reactive, transient
416 species that is produced primarily by microbial reduction of nitrate. In anaerobic aquifers with
417 relatively high nitrate concentrations, the production of nitrite by nitrate-reducing
418 microorganisms, together with enzymatically catalyzed, nitrate-dependent U(IV) oxidation, are
419 likely dual processes by which reduced U solids may be oxidized and mobilized in the aqueous
420 phase. Steady-state dissolution rates appear to be controlled by U(VI) detachment and release
421 to solution as the rate-determining step once surface-oxidized U(VI) species form on UO₂(s)
422 particle surfaces. Initial dissolution rates, which were not considered in this study and may
423 involve release of both U(IV) and U(VI) species, are more likely to be controlled by electron-
424 transfer processes involving microbial enzymatic oxidation of U(IV) and reduction of nitrate,

425 and by surface adsorption, complexation, and U(IV) oxidation^{22,41}. If a steady-state
426 concentration of surface-oxidized U species develops, the overall rate of U release to solution
427 may be similar to that of uranyl oxyhydroxide minerals, and thus would be strongly controlled
428 by pH and dissolved carbonate concentration⁶². In natural groundwater, the presence of
429 dissolved inorganic carbon, an ubiquitous component of groundwater, would promote the
430 removal of surface U(VI) by formation of uranyl-carbonate complexes^{22,62}, increasing U
431 mobility. Our findings improve our understanding of U(IV) oxidation and remobilization
432 processes in nitrate-contaminated aquifers, and will contribute to predictive modeling and
433 strategies for mitigating U mobilization.

434

435

436 **ASSOCIATED CONTENT**

437 **Supporting Information**

438 Supporting information is available free of charge via the Internet at <http://pubs.acs.org>.

439 Methods; Figure S1, XRD biogenic UO₂(s); Figure S2, SEM and TEM images of biogenic
440 UO₂(s); Figure S3, Log UO₂(s) dissolution rate vs. influent nitrite concentration; Figure S4,
441 nitrite effluent concentrations in the experiments performed in the presence of *T. denitrificans*
442 and nitrate; Figure S5, Uranium L_{III} XANES spectra and LCF of the first derivative of spectra;
443 Table S1, experimental conditions for dissolution experiments and solid analyses performed
444 before and after reaction; Table S2, experimental conditions and UO₂(s) dissolution rates based
445 on steady-state values; Table S3, uranium L_{III} EXAFS fit results of biogenic UO₂(s) spectra;
446 Table S4, uranium L_{III} EXAFS fit results of reference compound spectra; Table S5, stability
447 constants for selected U(IV) complexes.

448

449 **AUTHOR INFORMATION**

450 **Corresponding author**

451 *E-mail: Maria-Pilar.Asta-Andres@univ-grenoble-alpes.fr

452 **Notes**

453 The authors declare no competing financial interest.

454

455 **ACKNOWLEDGMENTS**

456 This study was supported by the Subsurface Biogeochemistry Research Program, U.S.
457 Department of Energy, Office of Science, Office of Biological and Environmental Research
458 [award number DE-AC02-05CH11231 (LBNL) and DE-FG02-08ER6414 (UC Merced)].
459 Portions of this research were carried out at the Stanford Synchrotron Radiation Lightsource at
460 the SLAC National Accelerator Laboratory, an Office of Science User Facility operated for the
461 U.S. Department of Energy Office of Science by Stanford University. Use of the Stanford
462 Synchrotron Radiation Lightsource, SLAC National Accelerator Laboratory, is supported by
463 the U.S. Department of Energy, Office of Science, Office of Basic Energy Sciences under
464 Contract No. DE-AC02-76SF00515. Maria P. Asta has received financial support from the
465 European Commission through the Marie Skłodowska-Curie Research Fellowship Programme.
466 We thank Peng Zhou, Nelson Rivera, Virginia Illera, Harshani Peiris, Jesus Luna, Jesus Ciriza,
467 Chi-Shuo Chen, Kennedy Nguyen, Gayatri Premshkharan, Masakazu Kanematsu, and Estela
468 Reinoso Maset for assistance. Thanks to M. Dunlap, Imaging and Microscopy Facility (UC
469 Merced), for assistance with XRD and electron microscopy, and to L. Zhao, Environmental
470 Analytical Laboratory (UC Merced), for analytical support.

471

472

473

474 **REFERENCES**

- 475 (1) Lovley, D.; Phillips, E.; Gorby, Y.; Landa, E. Microbial reduction of uranium. *Nature*
 476 **1991**, *350*, 413–416.
- 477 (2) Lovley, D.; Phillips, E. Reduction of uranium by *Desulfovibrio desulfuricans*. *Appl.*
 478 *Environ. Microbiol.* **1992**, *58* (3), 850–856.
- 479 (3) Williams, K. H.; Bargar, J. R.; Lloyd, J. R.; Lovley, D. R. Bioremediation of uranium-
 480 contaminated groundwater: A systems approach to subsurface biogeochemistry. *Curr.*
 481 *Opin. Biotechnol.* **2013**, *24* (3), 489–497.
- 482 (4) Anderson, R. T.; Vrionis, H. A.; Ortiz-bernad, I.; Resch, C. T.; Long, P. E.; Dayvault,
 483 R.; Karp, K.; Marutzky, S.; Metzler, D. R.; Peacock, A.; White, D.C.; Lowe, M.; Lovley,
 484 D.R. Stimulating the in situ activity of *Geobacter* species to remove uranium from the
 485 groundwater of a uranium-contaminated aquifer. *Appl. Environ. Microbiol.* **2003**, *69*
 486 (10), 5884–5891.
- 487 (5) Alessi, D. S.; Lezama-Pacheco, J. S.; Janot, N.; Suvorova, E. I.; Cerrato, J. M.; Giammar,
 488 D. E.; Davis, J. A.; Fox, P. M.; Williams, K. H.; Long, P. E.; Handley, K.M.; Bernier-
 489 Latmani, R.; Bargar, J.R. Speciation and reactivity of uranium products formed during
 490 in situ bioremediation in a shallow alluvial aquifer. *Environ. Sci. Technol.* **2014**, *48* (21),
 491 12842–12850.
- 492 (6) Schofield, E. J.; Veeramani, H.; Sharp, J. O.; Suvorova, E.; Bernier-Latmani, R.; Mehta,
 493 A.; Stahlman, J.; Webb, S. M.; Clark, D. L.; Conradson, S. D.; Ilton, E.; Bargar, J.R.
 494 Structure of biogenic uraninite produced by *Shewanella oneidensis* Strain MR-1.
 495 *Environ. Sci. Technol.* **2008**, *42* (21), 7898–7904.
- 496 (7) Burgos, W. D.; McDonough, J. T.; Senko, J. M.; Zhang, G.; Dohnalkova, A. C.; Kelly,
 497 S. D.; Gorby, Y.; Kemner, K. M. Characterization of uraninite nanoparticles produced
 498 by *Shewanella oneidensis* MR-1. *Geochim. Cosmochim. Acta* **2008**, *72* (20), 4901–4915.
 499 <https://doi.org/10.1016/j.gca.2008.07.016>.
- 500 (8) Bernier-Latmani, R.; Veeramani, H.; Vecchia, E. D.; Junier, P.; Lezama-Pacheco, J. S.;
 501 Suvorova, E. I.; Sharp, J. O.; Wigginton, N. S.; Bargar, J. R. Non-uraninite products of
 502 microbial U(VI) reduction. *Environ. Sci. Technol.* **2010**, *44* (24), 9456–9462.
- 503 (9) Sharp, J. O.; Lezama-Pacheco, J. S.; Schofield, E. J.; Junier, P.; Ulrich, K.-U.; Chinni,
 504 S.; Veeramani, H.; Margot-Roquier, C.; Webb, S. M.; Tebo, B. M.; Giammar, D.E.;
 505 Bargar, J. R.; Bernier-Latmani, R. Uranium speciation and stability after reductive
 506 immobilization in aquifer sediments. *Geochim. Cosmochim. Acta* **2011**, *75* (21), 6497–
 507 6510.
- 508 (10) Loreggian, L.; Sorwat, J.; Byrne, J. M.; Kappler, A.; Bernier-Latmani, R. Role of iron
 509 sulfide phases in the stability of noncrystalline tetravalent uranium in sediments.
 510 *Environ. Sci. Technol.* **2020**.
- 511 (11) Kelly, S. D.; Kemner, K. M.; Carley, J.; Criddle, C.; Jardine, P. M.; Marsh, T. L.;
 512 Phillips, D.; Watson, D.; Wu, W.-M. Speciation of uranium in sediments before and after
 513 in situ biostimulation. *Environ. Sci. Technol.* **2008**, *42* (5), 1558–1564.
- 514 (12) Bargar, J. R.; Williams, K. H.; Campbell, K. M.; Long, P. E.; Stubbs, J. E.; Suvorova, E.

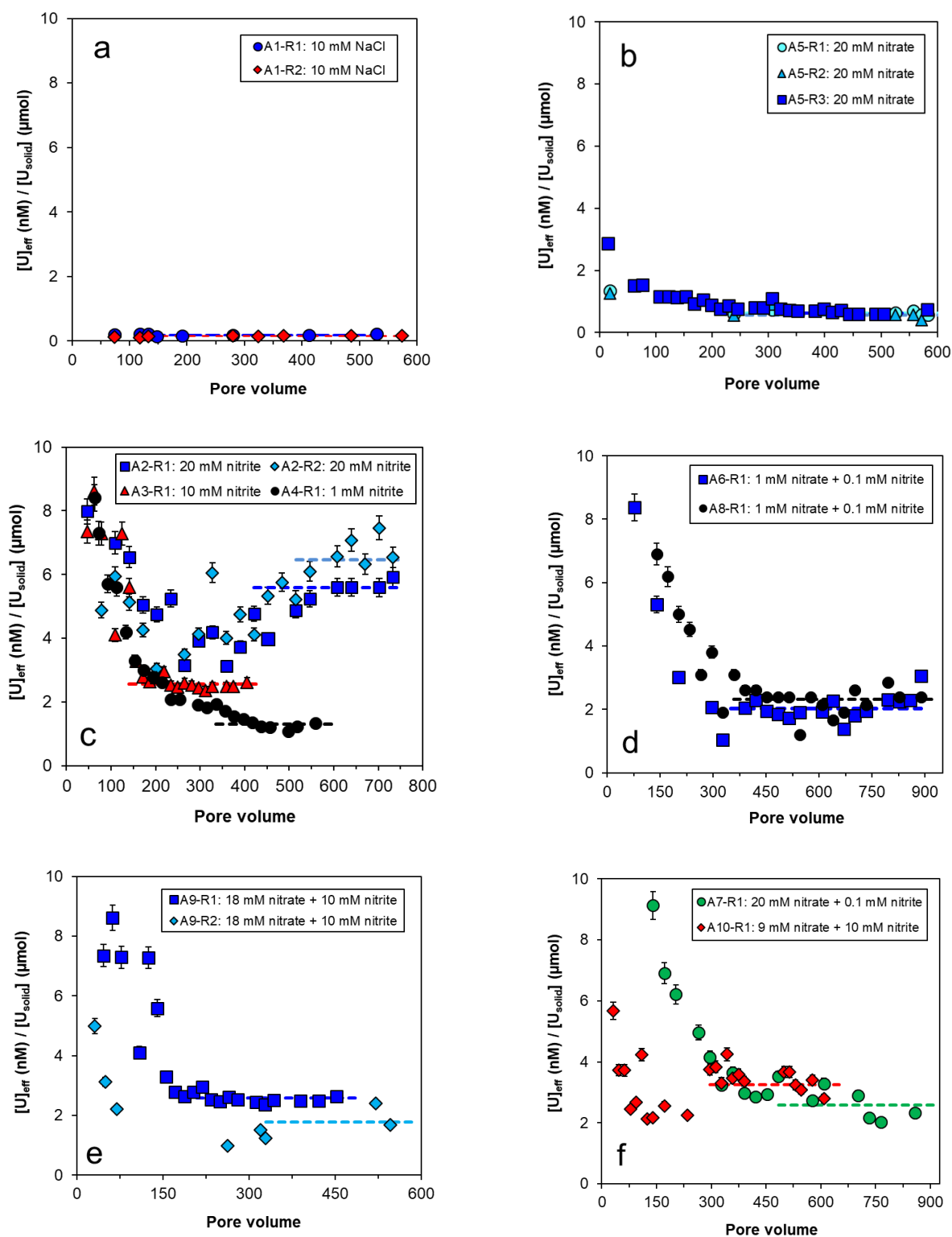
- 515 I.; Lezama-Pacheco, J. S.; Alessi, D. S.; Stylo, M.; Webb, S. M.; Davis, J.A.; Giammar,
516 D.E.; Blue, L.Y.; Bernier-Latmani, R. Uranium redox transition pathways in acetate-
517 amended sediments. *Proc. Natl. Acad. Sci. U. S. A.* **2013**, *110* (12), 4506–4511.
- 518 (13) Stoliker, D. L.; Campbell, K. M.; Fox, P. M.; Singer, D. M.; Kaviani, N.; Carey, M.;
519 Peck, N. E.; Bargar, J. R.; Kent, D. B.; Davis, J. A. Evaluating chemical extraction
520 techniques for the determination of uranium oxidation state in reduced aquifer sediments.
521 *Environ. Sci. Technol.* **2013**, *47* (16), 9225–9232.
- 522 (14) Newsome, L.; Morris, K.; Shaw, S.; Trivedi, D.; Lloyd, J. R. The stability of microbially
523 reduced U(IV); impact of residual electron donor and sediment ageing. *Chem. Geol.*
524 **2015**, *409*, 125–135.
- 525 (15) Kelly, S. D.; Wu, W. M.; Yang, F.; Criddle, C. S.; Marsh, T. L.; O’Loughlin, E. J.; Ravel,
526 B.; Watson, D.; Jardine, P. M.; Kemner, K. M. Uranium transformations in static
527 microcosms. *Environ. Sci. Technol.* **2010**, *44* (1), 236–242.
- 528 (16) Finneran, K. T.; Housewright, M. E.; Lovley, D. R. Multiple influences of nitrate on
529 uranium solubility during bioremediation of uranium-contaminated subsurface
530 sediments. *Environ. Microbiol.* **2002**, *4* (9), 510–516.
- 531 (17) Senko, J. M.; Istok, J. D.; Suflita, J. M.; Krumholz, L. R. In-situ evidence for uranium
532 immobilization and remobilization. *Environ. Sci. Technol.* **2002**, *36* (7), 1491–1496.
- 533 (18) Beller, H. H. R. Anaerobic, nitrate-dependent oxidation of U(IV) oxide minerals by the
534 chemolithoautotrophic bacterium *Thiobacillus denitrificans*. *Appl. Environ. Microbiol.*
535 **2005**, *71* (Iv), 2170–2174.
- 536 (19) Wan, J.; Tokunaga, T. K.; Brodie, E.; Wang, Z.; Zheng, Z.; Herman, D.; Hazen, T. C.;
537 Firestone, M. K.; Sutton, S. R. Reoxidation of bioreduced uranium under reducing
538 conditions. *Environ. Sci. Technol.* **2005**, *39* (16), 6162–6169.
- 539 (20) Moon, H. S.; Komlos, J.; Jaffé, P. R. Uranium reoxidation in previously bioreduced
540 sediment by dissolved oxygen and nitrate. *Environ. Sci. Technol.* **2007**, *41* (13), 4587–
541 4592.
- 542 (21) Singh, G.; Şengör, S. S.; Bhalla, A.; Kumar, S.; De, J.; Stewart, B.; Spycher, N.; Ginn,
543 T. M.; Peyton, B. M.; Sani, R. K. Reoxidation of biogenic reduced uranium: A challenge
544 toward bioremediation. *Crit. Rev. Environ. Sci. Technol.* **2014**, *44* (4), 391–415.
- 545 (22) Ulrich, K.-U.; Ilton, E. S.; Veeramani, H.; Sharp, J. O.; Bernier-Latmani, R.; Schofield,
546 E. J.; Bargar, J. R.; Giammar, D. E. Comparative dissolution kinetics of biogenic and
547 chemogenic uraninite under oxidizing conditions in the presence of carbonate. *Geochim.*
548 *Cosmochim. Acta* **2009**, *73* (20), 6065–6083.
- 549 (23) Cerrato, J. M.; Ashner, M. N.; Alessi, D. S.; Lezama-Pacheco, J. S.; Bernier-Latmani,
550 R.; Bargar, J. R.; Giammar, D. E. Relative reactivity of biogenic and chemogenic
551 uraninite and biogenic noncrystalline U(IV). *Environ. Sci. Technol.* **2013**, *47* (17), 9756–
552 9763.
- 553 (24) Riley, R. G.; Zachara, J. M. *Nature of Chemical Contamination on DOE Lands and*
554 *Identification of Representative Contaminant Mixtures for Basic Subsurface Science*
555 *Research.*; Washington, DC, 1992.

- 556 (25) Spain, A. M.; Krumholz, L. R. Nitrate-reducing bacteria at the nitrate and radionuclide
557 contaminated Oak Ridge Integrated Field Research Challenge Site: A review.
558 *Geomicrobiol. J.* **2011**, *28* (5–6), 418–429.
- 559 (26) Lloyd, J. R.; Renshaw, J. C. Bioremediation of radioactive waste: Radionuclide–microbe
560 interactions in laboratory and field-scale studies. *Curr. Opin. Biotechnol.* **2005**, *16* (3),
561 254–260.
- 562 (27) Smith, M. B.; Rocha, A. M.; Smillie, C. S.; Olesen, S. W.; Paradis, C.; Wu, L.; Campbell,
563 J. H.; Fortney, J. L.; Mehlhorn, T. L.; Lowe, K. A.; Earles, J.E.; Phillips, J.; Techtmann,
564 S. M.; Joyner, D.C.; Elias, D.A.; Dwayne, A.; Bailey, K. L.; Hurt, R.A.; Preheim, S. P.;
565 Sanders, M. C.; Yang, J.; Mueller, M. A.; Brooks, S.; Watson, D. B.; Zhang, P.; He, Z.;
566 Dubinsky, E.A.; Adams, P.D.; Arkin, A.P.; Fields, M.W.; Zhou, J.; Alm, E.J.; Hazen, T.
567 C. Natural bacterial communities serve as quantitative geochemical biosensors. *MBio*
568 **2015**, *6* (3), e00326-15.
- 569 (28) Van Berk, W.; Fu, Y. Redox roll-front mobilization of geogenic uranium by nitrate input
570 into aquifers: Risks for groundwater resources. *Environ. Sci. Technol.* **2017**, *51* (1), 337–
571 345.
- 572 (29) Banning, A.; Demmel, T.; Rude, T. R.; Wrobel, M. Groundwater uranium origin and fate
573 control in a river valley aquifer. *Environ. Sci. Technol.* **2013**, *47* (24), 13941–13948.
- 574 (30) Nolan, J.; Weber, K. A. Natural uranium contamination in major U.S. aquifers linked to
575 nitrate. *Environ. Sci. Technol. Lett.* **2015**, *2* (8), 215–220.
- 576 (31) Senko, J. M.; Mohamed, Y.; Dewers, T. A.; Krumholz, L. R. Role for Fe(III) minerals
577 in nitrate-dependent microbial U(IV) oxidation. *Environ. Sci. Technol.* **2005**, *39* (8),
578 2529–2536.
- 579 (32) Beller, H. R.; Chain, P. S. G.; Letain, T. E.; Chakicherla, A.; Larimer, F. W.; Richardson,
580 P. M.; Coleman, M. A.; Wood, A. P.; Kelly, D. P. The genome sequence of the obligately
581 chemolithoautotrophic, facultatively anaerobic bacterium *Thiobacillus denitrificans*. *J.*
582 *Bacteriol.* **2006**, *188* (4), 1473–1488.
- 583 (33) Straub, K. L.; Benz, M.; Schink, B.; Widdel, F. Anaerobic, nitrate-dependent microbial
584 oxidation of ferrous iron. *Appl. Environ. Microbiol.* **1996**, *62* (4), 1458–1460.
- 585 (34) Torrentó, C.; Cama, J.; Urmeneta, J.; Otero, N.; Soler, A. Denitrification of groundwater
586 with pyrite and *Thiobacillus denitrificans*. *Chem. Geol.* **2010**, *278* (1–2), 80–91.
- 587 (35) Beller, H. R.; Zhou, P.; Legler, T. C.; Chakicherla, A.; Kane, S.; Letain, T. E.; O’Day,
588 P. A. Genome-enabled studies of anaerobic, nitrate-dependent iron oxidation in the
589 chemolithoautotrophic bacterium *Thiobacillus denitrificans*. *Front. Microbiol.* **2013**, *4*,
590 249.
- 591 (36) Beller, H. R.; Letain, T. E.; Chakicherla, A.; Kane, S. R.; Legler, T. C.; Coleman, M. A.
592 Whole-genome transcriptional analysis of chemolithoautotrophic thiosulfate oxidation
593 by *Thiobacillus denitrificans* under aerobic versus denitrifying conditions. *J. Bacteriol.*
594 **2006**, *188* (19), 7005–7015.
- 595 (37) Wu, W.-M.; Carley, J.; Green, S. J.; Luo, J.; Kelly, S. D.; Van Nostrand, J.; Lowe, K.;
596 Mehlhorn, T.; Carroll, S.; Boonchayanant, B.; Ofler, Löffler, F. E.; Watson, D.; Kemner,
597 K. M.; Zhou, J.; Kitanidis, P. K.; Kostka, J. E.; Jardine, P. M.; Criddle, C. S. Effects of

- 598 nitrate on the stability of uranium in a bioreduced region of the subsurface. *Environ. Sci.*
599 *Technol.* **2010**, *44* (13), 5104–5111.
- 600 (38) Beller, H. R.; Legler, T. C.; Bourguet, F.; Letain, T. E.; Kane, S. R.; Coleman, M. A.
601 Identification of *c*-type cytochromes involved in anaerobic, bacterial U(IV) oxidation.
602 *Biodegradation* **2009**, *20* (1), 45–53.
- 603 (39) Bruno, J.; Casas, I.; Puigdomènech, I. UO₂ under reducing conditions and the influence
604 of an oxidized surface layer (UO_{2+x}): Application of a continuous flow-through reactor.
605 *Geochim. Cosmochim. Acta* **1991**, *55* (1), 647–658.
- 606 (40) Giménez, J.; Clarens, F.; Casas, I.; Rovira, M.; de Pablo, J.; Bruno, J. Oxidation and
607 dissolution of UO₂ in bicarbonate media: Implications for the spent nuclear fuel oxidative
608 dissolution mechanism. *J. Nucl. Mater.* **2005**, *345* (2–3), 232–238.
- 609 (41) Ulrich, K.-U.; Singh, A.; Schofield, E. J.; Bargar, J. R.; Veeramani, H.; Sharp, J. O.;
610 Bernier-Latmani, R.; Giammar, D. E. Dissolution of biogenic and synthetic UO₂ under
611 varied reducing conditions. *Environ. Sci. Technol.* **2008**, *42* (15), 5600–5606.
- 612 (42) Frazier, S. W.; Kretzschmar, R.; Kraemer, S. M. Bacterial siderophores promote
613 dissolution of UO₂ under reducing conditions. *Environ. Sci. Technol.* **2005**, *39* (15),
614 5709–5715.
- 615 (43) Handley-Sidhu, S.; Bryan, N. D.; Worsfold, P. J.; Vaughan, D. J.; Livens, F. R.; Keith-
616 Roach, M. J. Corrosion and transport of depleted uranium in sand-rich environments.
617 *Chemosphere* **2009**, *77* (10), 1434–1439.
- 618 (44) Veeramani, H.; Schofield, E. J.; Sharp, J. O.; Suvorova, E. I.; Ulrich, K.-U.; Mehta, A.;
619 Giammar, D. E.; Bargar, J. R.; Bernier-Latmani, R. Effect of Mn(II) on the structure and
620 reactivity of biogenic uraninite. *Environ. Sci. Technol.* **2009**, *43* (17), 6541–6547.
- 621 (45) Bi, Y.; Stylo, M.; Bernier-Latmani, R.; Hayes, K. F. Rapid Mobilization of
622 noncrystalline U(IV) coupled with FeS oxidation. *Environ. Sci. Technol.* **2016**, *50* (3),
623 1403–1411.
- 624 (46) Fredrickson, J. K.; Zachara, J. M.; Kennedy, D. W.; Duff, M. C.; Gorby, Y. A.; Li, S. M.
625 W.; Krupka, K. M. Reduction of U(VI) in Goethite (α -FeOOH) Suspensions by a
626 dissimilatory metal-reducing bacterium. *Geochim. Cosmochim. Acta* **2000**, *64* (18),
627 3085–3098.
- 628 (47) Pierce, E. M.; Icenhower, J. P.; Serne, R. J.; Catalano, J. G. Experimental Determination
629 of UO₂(Cr) dissolution kinetics: Effects of solution saturation state and pH. *J. Nucl.*
630 *Mater.* **2005**, *345* (2–3), 206–218.
- 631 (48) Allen, P. G.; Shuh, D. K.; Bucher, J. J.; Edelstein, N. M.; Palmer, C. E. A.; Silva, R. J.;
632 Nguyen, S. N.; Marquez, L. N.; Hudson, E. A. Determination of uranium structures by
633 EXAFS: Schoepite and other U(VI) oxide precipitates. *Radiochim. Acta* **1996**, *75*, 47–
634 53.
- 635 (49) Chakraborty, S.; Favre, F.; Banerjee, D.; Scheinost, A. C.; Mullet, M.; Ehrhardt, J.-J.;
636 Brendle, J.; Vidal, L.; Charlet, L. U(VI) Sorption and reduction by Fe(II) sorbed on
637 montmorillonite. *Environ. Sci. Technol.* **2010**, *44* (10), 3779–3785.
- 638 (50) Alessi, D. S.; Uster, B.; Veeramani, H.; Suvorova, E. I.; Lezama-Pacheco, J. S.; Stubbs,

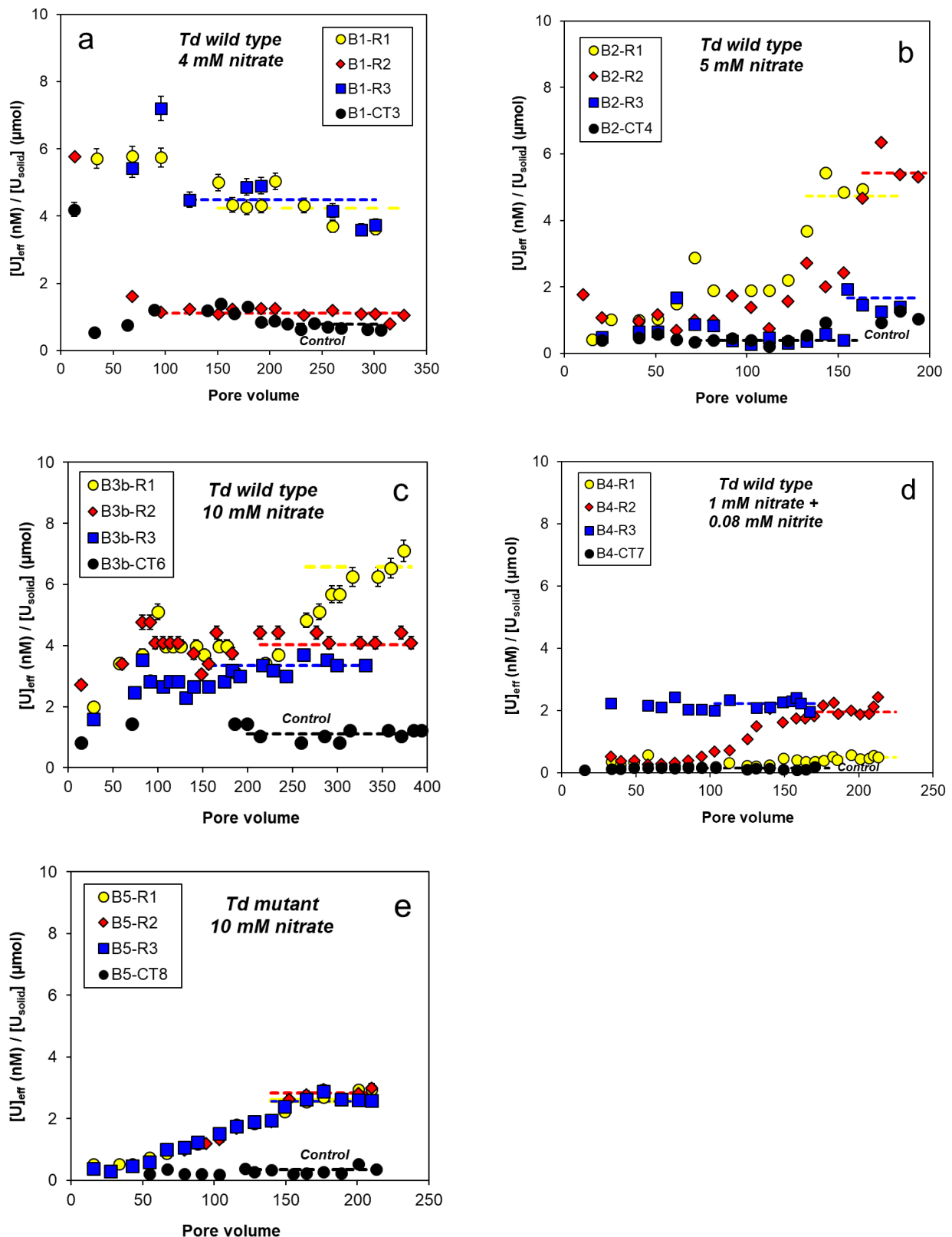
- 639 J. E.; Bargar, J. R.; Bernier-Latmani, R. ESI-Quantitative separation of monomeric
640 U(IV) from UO₂ in products of U(VI) reduction. *Environ. Sci. Technol.* **2012**, *46* (11),
641 6150–6157.
- 642 (51) Boyanov, M. I.; Fletcher, K. E.; Kwon, M. J.; Rui, X.; O’Loughlin, E. J.; Löffler, F. E.;
643 Kemner, K. M. Solution and microbial controls on the formation of reduced U(IV)
644 species. *Environ. Sci. Technol.* **2011**, *45* (19), 8336–8344.
- 645 (52) Morin, G.; Mangeret, A.; Othmane, G.; Stetten, L.; Seder-Colomina, M.; Brest, J.; Ona-
646 Nguema, G.; Bassot, S.; Courbet, C.; Guillevic, J.; Thouvenot, A.; Mathon, O.; Proux,
647 O.; Bargar, J.R. Mononuclear U(IV) complexes and ningyoite as major uranium species
648 in lake sediments. *Geochemical Perspect. Lett.* **2016**, No. Iv, 95–105.
- 649 (53) Stetten, L.; Mangeret, A.; Brest, J.; Seder-Colomina, M.; Le Pape, P.; Ikogou, M.; Zeyen,
650 N.; Thouvenot, A.; Julien, A.; Alcalde, G.; Reyss, J. L.; Bombléd, B.; Rabouille, C.;
651 Olivi, L.; Proux, O.; Cazala, C.; Morin, G. Geochemical control on the reduction of
652 U(VI) to mononuclear U(IV) species in lacustrine sediments. *Geochim. Cosmochim.*
653 *Acta* **2018**, *222*, 171–186.
- 654 (54) Stetten, L.; Blanchart, P.; Mangeret, A.; Lefebvre, P.; Le Pape, P.; Brest, J.; Merrot, P.;
655 Julien, A.; Proux, O.; Webb, S. M.; Bargar, J. R.; Cazala, C.; Morin, G. Redox
656 Fluctuations and organic complexation govern uranium redistribution from U(IV)-
657 phosphate minerals in a mining-polluted wetland soil, Brittany, France. *Environ. Sci.*
658 *Technol.* **2018**, *52* (22), 13099–13109.
- 659 (55) Mikutta, C.; Langner, P.; Bargar, J. R.; Kretzschmar, R. Tetra- and hexavalent Uranium
660 forms bidentate-mononuclear complexes with particulate organic matter in a naturally
661 uranium-enriched peatland. *Environ. Sci. Technol.* **2016**, *50* (19), 10465–10475.
- 662 (56) Shoesmith, D. W. Fuel corrosion processes under waste disposal conditions. *J. Nucl.*
663 *Mater.* **2000**, *282* (1), 1–31.
- 664 (57) Santos, B. G.; Nesbitt, H. W.; Noël, J. J.; Shoesmith, D. W. X-Ray Photoelectron
665 Spectroscopy Study of anodically oxidized SIMFUEL surfaces. *Electrochim. Acta* **2004**,
666 *49* (11), 1863–1873.
- 667 (58) Santos, B. G.; Noël, J. J.; Shoesmith, D. W. The effect of pH on the anodic dissolution
668 of SIMFUEL (UO₂). *J. Electroanal. Chem.* **2006**, *586* (1), 1–11.
- 669 (59) Christensen, H.; Sunder, S.; Shoesmith, D. W. Oxidation of Nuclear Fuel (UO₂) by the
670 products of water radiolysis: Development of a kinetic model. *J. Alloys Compd.* **1994**,
671 *213–214* (C), 93–99.
- 672 (60) Hatakeyama, K.; Park, Y.; Tomiyasu, H. Photo-enhancement effect on oxidation
673 reaction of Uranium(IV) by NO₃⁻ in perchloric acid solutions. *J. Nucl. Sci. Technol.*
674 **1997**, *34* (7), 695–699.
- 675 (61) Giammar, D. E.; Cerrato, J. M.; Mehta, V.; Wang, Z.; Wang, Y.; Pepping, T. J.; Ulrich,
676 K.-U.; Lezama-Pacheco, J. S.; Bargar, J. R. Effect of diffusive transport limitations on
677 UO₂ dissolution. *Water Res.* **2012**, *46* (18), 6023–6032.
- 678 (62) Reinoso-Maset, E.; Steefel, C. I.; Um, W.; Chorover, J.; O’Day, P. A. Rates and
679 mechanisms of uranyl oxyhydroxide mineral dissolution. *Geochim. Cosmochim. Acta*
680 **2017**, *207* (September 2018), 298–321.

- 681 (63) Pérez, I.; Casas, I.; Martín, M.; Bruno, J. The thermodynamics and kinetics of
682 uranophane dissolution in bicarbonate test solutions. *Geochim. Cosmochim. Acta* **2000**,
683 *64* (4), 603–608.
- 684 (64) Ilton, E. S.; Liu, C.; Yantasee, W.; Wang, Z.; Moore, D. A.; Felmy, A. R.; Zachara, J.
685 M. The dissolution of synthetic Na-Boltwoodite in sodium carbonate solutions.
686 *Geochim. Cosmochim. Acta* **2006**, *70* (19), 4836–4849.
- 687 (65) Gudavalli, R. K. P.; Katsenovich, Y. P.; Wellman, D. M.; Idarraga, M.; Lagos, L. E.;
688 Tansel, B. Comparison of the kinetic rate law parameters for the dissolution of natural
689 and synthetic autunite in the presence of aqueous bicarbonate ions. *Chem. Geol.* **2013**,
690 *351*, 299–309.
- 691 (66) Spycher, N. F.; Issarangkun, M.; Stewart, B. D.; Sevinç Şengör, S.; Belding, E.; Ginn,
692 T. R.; Peyton, B. M.; Sani, R. K. Biogenic uraninite precipitation and its reoxidation by
693 Iron(III) (Hydr)Oxides: A reaction modeling approach. *Geochim. Cosmochim. Acta*
694 **2011**, *75* (16), 4426–4440.
- 695 (67) Newsome, L.; Morris, K.; Lloyd, J. R. The Biogeochemistry and Bioremediation of
696 uranium and other priority radionuclides. *Chem. Geol.* **2014**, *363*, 164–184.
- 697 (68) Casas, I.; Giménez, J.; Marti, V.; Torrero, M. E.; Pablo, J. de. Kinetic Studies of
698 Unirradiated UO₂ Dissolution under oxidizing conditions in batch and flow experiments.
699 *Radiochim. Acta* **1994**, *66–67* (s1), 23–27.
- 700 (69) Bruno J., Casas I., Cera E., De Pablo J., G. J. and T. M. E. Uranium (IV) dioxide and
701 SIMFUEL as chemical analogues of nuclear spent fuel matrix dissolution. A compar-
702 ison of dissolution results in a standard NaCl/NaHCO₃ solution. *Sci. Basis Nucl. Waste*
703 *Manag. XVII.* **1995**, *Symposium*, 601–608.
- 704 (70) Mailloux, B. J.; Kim, C.; Kichuk, T.; Nguyen, K.; Precht, C.; Wang, S.; Jewell, T. N.
705 M.; Karaoz, U.; Brodie, E. L.; Williams, K. H.; Beller, H. R.; Buchholz, B. A. Paired
706 RNA radiocarbon and sequencing analyses indicate the importance of autotrophy in a
707 shallow alluvial aquifer. *Sci. Rep.* **2019**, *9*, 10370.
- 708 (71) Cardenas, E.; Wu, W. M.; Leigh, M. B.; Carley, J.; Carroll, S.; Gentry, T.; Luo, J.;
709 Watson, D.; Gu, B.; Ginder-Vogel, M.; Kitanidis, P. K.; Jardine, P. M.; Zhou, J.; Criddle,
710 C. S.; Marsh, T. L.; Tiedje, J. M. Microbial communities in contaminated sediments,
711 associated with bioremediation of uranium to submicromolar levels. *Appl. Environ.*
712 *Microbiol.* **2008**, *74* (12), 3718–3729.
- 713
- 714



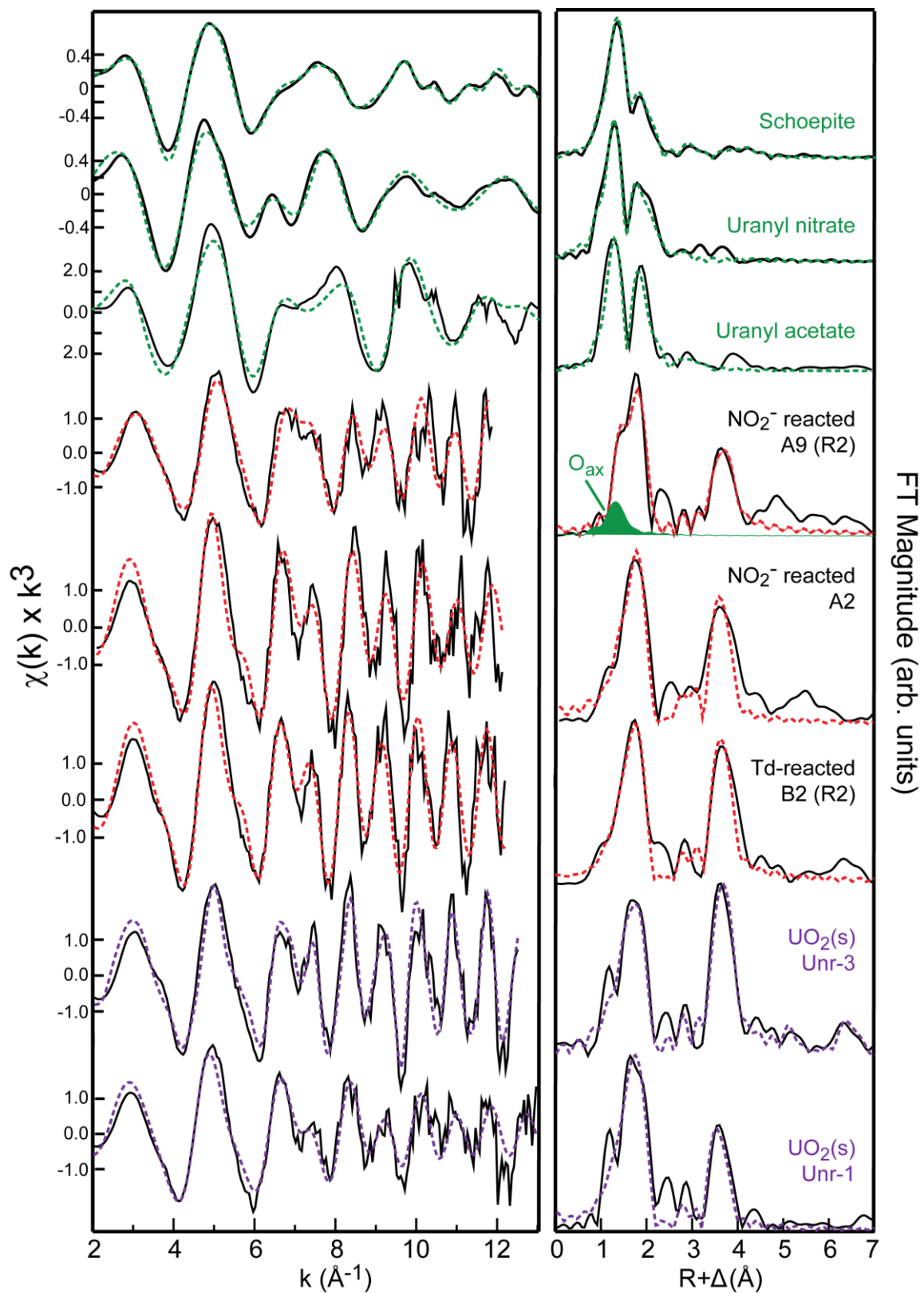
715 **Figure 1.** Uranium released in column experiments normalized by the initial U mass as a
 716 function of pore volume (a) without oxidant; (b) with NO_3^- ; (c) with NO_2^- ; and (d-f) with a
 717 mixture of NO_3^- and NO_2^- . Error bars correspond to the analytical uncertainty in measured U
 718 concentration. Dashed lines represent the steady-state values for each experiment used to
 719 calculate U dissolution rate. Initial flush-out of high U is not shown.

720



721 **Figure 2.** Uranium released in column experiments normalized by the initial U mass as a function
 722 of pore volume in the presence of wild-type *T. denitrificans* and (a) 4 mM NO_3^- ; (b) 5 mM NO_3^- (c)
 723 10 mM NO_3^- ; (d) 1 mM NO_3^- and 0.08 mM NO_2^- ; and (e) 10 mM NO_3^- and a *T. denitrificans*
 724 mutant strain (*Tbd_0187::kan*) ~50% defective in U(IV) oxidation compared to simultaneous abiotic control
 725 experiments without *T. denitrificans* (black circles). Error bars correspond to the analytical

726 uncertainty in measured U concentration. Dashed lines represent the steady-state values for each
727 experiment used to calculate U dissolution rate. Initial flush-out of high U is not shown.
728

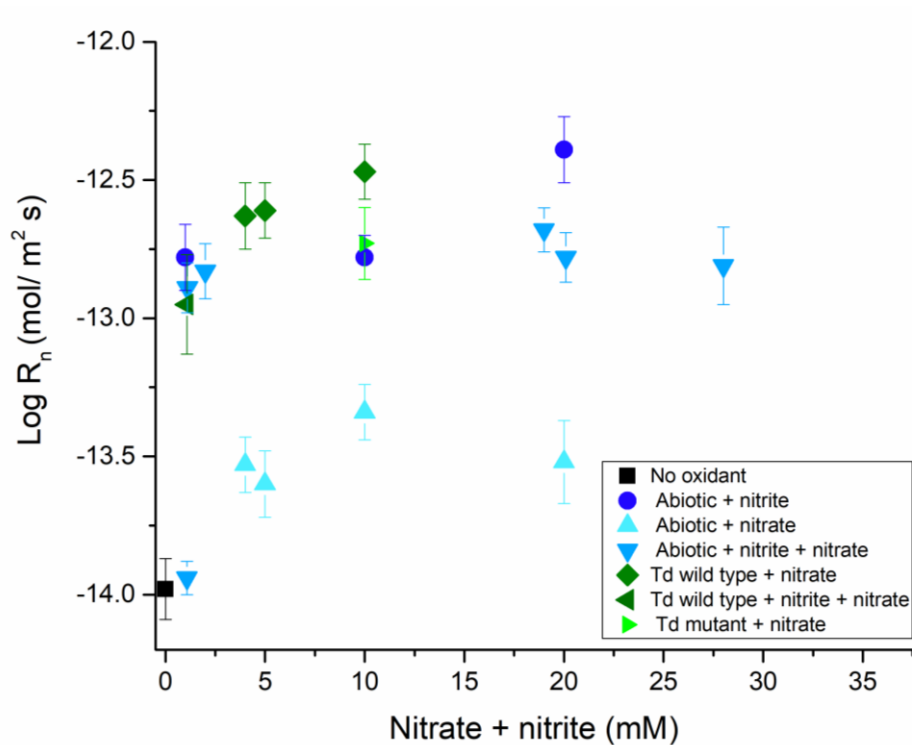


729

730
731
732
733

Figure 3. Uranium L_{III} EXAFS spectra and Fourier Transforms (FT) of unreacted UO₂(s) samples (Unr-1, Unr-3), reacted samples (B2(R2), A2, A9(R2)), and U(VI) reference compounds (uranyl acetate, uranyl nitrate, schoepite). Overlapping dashed lines represent the non-linear least-squares shell-by-shell fits (numerical fit results shown in Tables S4 and S5).

734



735
736

737 **Figure 4.** Log UO₂(s) dissolution rate vs. oxidant concentration (no oxidant, black squares;
738 NO₂⁻, NO₃⁻, or a mixture of NO₃⁻ and NO₂⁻) in the absence (abiotic experiments, blue symbols)
739 or presence of *T. denitrificans* (Td wild type and Td mutant, green symbols). Error was
740 estimated by propagation of experimental uncertainties and dominated by the variation in
741 effluent U concentration at steady state ($[U]_{ss} \leq 15\%$), and the uncertainty of the U mass
742 measurements (0.5-25%).

1 **Table 1.** Experiment type, influent solutions, and UO₂(s) dissolution rates obtained in this work and previous studies under anaerobic conditions.

UO ₂ (s)	type of experiment	pH	influent electrolyte	Rate (mol m ⁻² s ⁻¹)	log Rate	experiment	replicates	reference
bio-UO ₂	flow-through column	7.0-7.3	10 mM NaCl	$1.05 \cdot 10^{-14} \pm 2.67 \cdot 10^{-15}$	-13.98±0.11	A1	R1, R2	<i>This work</i>
			<i>abiotic</i> , 1 mM NO ₂ ⁻	$1.66 \cdot 10^{-13} \pm 3.81 \cdot 10^{-14}$	-12.78±0.10	A4	R1	
			<i>abiotic</i> , 10 mM NO ₂ ⁻	$1.64 \cdot 10^{-13} \pm 2.98 \cdot 10^{-14}$	-12.78±0.08	A3	R1	
			<i>abiotic</i> , 20 mM NO ₂ ⁻	$4.11 \cdot 10^{-13} \pm 1.11 \cdot 10^{-13}$	-12.39±0.12	A2	R1, R2	
			<i>abiotic</i> , 1 mM NO ₃ ⁻ + 0.1 mM NO ₂ ⁻	$1.30 \cdot 10^{-13} \pm 2.61 \cdot 10^{-14}$	-12.89±0.09	A6	R1	
			<i>abiotic</i> , 1 mM NO ₃ ⁻ + 1 mM NO ₂ ⁻	$1.49 \cdot 10^{-13} \pm 3.33 \cdot 10^{-14}$	-12.83±0.10	A8	R1	
			<i>abiotic</i> , 20 mM NO ₃ ⁻ + 0.1 mM NO ₂ ⁻	$1.65 \cdot 10^{-13} \pm 2.62 \cdot 10^{-14}$	-12.78±0.09	A7	R1	
			<i>abiotic</i> , 9 mM NO ₃ ⁻ + 10 mM NO ₂ ⁻	$2.09 \cdot 10^{-13} \pm 4.09 \cdot 10^{-14}$	-12.67±0.08	A10	R1	
			<i>abiotic</i> , 18 mM NO ₃ ⁻ + 10 mM NO ₂ ⁻	$1.55 \cdot 10^{-13} \pm 4.71 \cdot 10^{-14}$	-12.81±0.14	A9	R1, R2	
			<i>abiotic</i> , 1 mM NO ₃ ⁻ + 0.08 mM NO ₂ ⁻	$1.15 \cdot 10^{-14} \pm 1.60 \cdot 10^{-15}$	-13.94±0.06	B4	CT7	
			<i>abiotic</i> , 4 mM NO ₃ ⁻	$2.93 \cdot 10^{-14} \pm 6.70 \cdot 10^{-15}$	-13.53±0.10	B1	CT3	
			<i>abiotic</i> , 5 mM NO ₃ ⁻	$2.51 \cdot 10^{-14} \pm 6.68 \cdot 10^{-15}$	-13.60±0.12	B2	CT4	
			<i>abiotic</i> , 10 mM NO ₃ ⁻	$4.61 \cdot 10^{-14} \pm 1.40 \cdot 10^{-14}$	-13.34±0.13	B3a, B3b, B5	CT5, CT6, CT8	
			<i>abiotic</i> , 20 mM NO ₃ ⁻	$3.02 \cdot 10^{-14} \pm 1.03 \cdot 10^{-14}$	-13.52±0.15	A5	R1, R2, R3	
			<i>Td</i> + 1 mM NO ₃ ⁻ + 0.08 mM NO ₂ ⁻	$1.12 \cdot 10^{-13} \pm 5.63 \cdot 10^{-14}$	-12.95±0.18	B4	R1, R2, R3	
			<i>Td</i> + 4 mM NO ₃ ⁻	$2.35 \cdot 10^{-13} \pm 8.06 \cdot 10^{-14}$	-12.63±0.12	B1	R1, R2, R3	
			<i>Td</i> + 5 mM NO ₃ ⁻	$2.44 \cdot 10^{-13} \pm 7.10 \cdot 10^{-14}$	-12.61±0.10	B2	R1, R2, R3	
<i>Td</i> + 10 mM NO ₃ ⁻	$3.41 \cdot 10^{-13} \pm 8.05 \cdot 10^{-14}$	-12.47±0.10	B3b	R1, R2, R3				
<i>Td mutant</i> + 10 mM NO ₃ ⁻	$1.91 \cdot 10^{-13} \pm 5.50 \cdot 10^{-14}$	-12.72±0.13	B5	R1, R2, R3				
synthetic UO ₂ ^a	flow-through	7-11	8 mM NaClO ₄	$1.90 \cdot 10^{-12}$	-11.72±0.02			Bruno et al. ³⁹
synthetic UO ₂	flow stirred tank reactor	7.50	10 mM NaClO ₄	$7.50 \cdot 10^{-13}$	-12.12±0.02			Frazier et al. ⁴²
bio-UO ₂	flow-through	7.60	1 mM HEPES	$9.85 \cdot 10^{-14}$	-13.01			Ulrich et al. ⁴¹
		7.25	1 mM HEPES	$3.42 \cdot 10^{-13}$	-12.47			
		7.67	1 mM HEPES	$1.07 \cdot 10^{-14}$	-13.97			
synthetic UO ₂	flow-through	8.00	1 mM NaNO ₃ , TAPS	$4.03 \cdot 10^{-12}$	-11.39			Ulrich et al. ⁴¹
		7.70	1 mM HEPES	$5.51 \cdot 10^{-13}$	-12.26			
		7.25	1 mM HEPES	$2.80 \cdot 10^{-13}$	-12.55			
		7.00	-	$2.15 \cdot 10^{-12}$	-11.72±0.24 ^b			

Td: *Thiobacillus denitrificans* wild type; *Td mutant*: *Thiobacillus denitrificans* mutant

^a a thin film was used

^b calculated at pH 7 from the kinetic rate law obtained by Ulrich et al.⁴¹ under reducing conditions for pH range 3-8

2

3

1 **Table 2.** Linear combination fit (LCF) results for U L_{III} XANES for a control experiment without
 2 oxidant (CT0), and for biogenic UO₂(s) samples after dissolution experiments under abiotic (*A*
 3 samples) conditions and in the presence of *T. denitrificans* (*B* samples). End-members used for LCF
 4 were biogenic UO₂(s) (unreacted sample Unr-1) for U(IV) and schoepite ((UO₂)₈O₂(OH)₁₂·12(H₂O))
 5 for U(VI).
 6

Sample	Oxidant	Model fit (%)			Goodness-of-fit ^a	Normalized fit (%) ^b	
		<i>U(IV)</i>	<i>U(VI)</i>	<i>Total</i>		<i>U(IV)</i>	<i>U(VI)</i>
CT0^c	no oxidant	100	0	100	0.002	100	0
A2	20 mM NO ₂	77	26	103	0.004	75	25
A5	20 mM NO ₃	98	0	98	0.004	100	0
A6	1 mM NO ₃ + 0.1 mM NO ₂	88	9	98	0.002	90	10
A8	1 mM NO ₃ + 1 mM NO ₂	89	13	102	0.002	88	12
A9(R2)	18 mM NO ₃ + 10 mM NO ₂	85	15	100	0.001	85	15
B1 (R1)	4 mM NO ₃	76	13	89	0.007	85	15
B1 (R2)	4 mM NO ₃	75	29	103	0.018	72	28
B2 (R1)	5 mM NO ₃	77	17	94	0.003	82	18
B2 (R2)	5 mM NO ₃	78	15	93	0.006	83	17
B3b (R1)	10 mM NO ₃	88	9	97	0.004	91	9
B3b (R2)	10 mM NO ₃	73	26	98	0.009	74	26

7 ^a R factor = $\Sigma(\text{data-fit})^2/\Sigma(\text{data})^2$

8 ^b The percentage of U components is normalized to a sum of 100%.

9 ^c Batch control experiment with biogenic UO₂(s) and 10 mM sodium acetate (no oxidant).

10
 11
 12
 13
 14
 15
 16
 17
 18